104 (2025) 105063

Contents lists available at ScienceDirect

Poultry Science

journal homepage: www.elsevier.com/locate/psj

CircFBLN2 regulates duck myoblast proliferation and differentiation through miR-22-5p and MEF2C interaction

Shuibing Liu [a,b,c], Jintao Wu [a,c], Hongxia Jiang [a,c], Ya'nan Zhou [a,c], Xuwen Huang [a,c], Yuxiang Wang [a,c], Zhanbin Xie [a], Zurong Liao [a,c], Zhenxvan Ding [a,c], Jing Liu [a,c], Xiaolong Hu [a,c], Huirong Mao [a,c], Sanfeng Liu [a,c], Biao Chen [a,c,*]

[a] College of Animal Science and Technology, Jiangxi Agricultural University, Nanchang 330045, Jiangxi, PR China
[b] College of Animal Science, South China Agricultural University, Guangzhou 510642, Guangdong, PR China
[c] Poultry Institute, Jiangxi Agricultural University, Nanchang 330045, PR China

ARTICLE INFO

Keywords:
Duck
skeletal muscle
circFBLN2
miR-22-5p
MEF2C

ABSTRACT

The growth and development of duck skeletal muscle significantly affect duck meat production, making it essential to understand the molecular mechanisms underlying these processes. Circular RNAs (circRNAs) and microRNAs (miRNAs) are identified in many species and play essential roles in the regulation of myogenic processes; however, research on circRNAs and miRNAs involved in the duck skeletal muscle development is limited. In prior whole-transcriptome RNA sequencing study, we identified differential expression of miR-22-5p and the novel circular RNA circFBLN2, which arises from the second exon of the *FBLN2* gene, in duck primary myoblasts (DPMs). In this study, we confirmed the circular structure of circFBLN2 and explored its expression patterns and functional implications in myogenesis. To elucidate the function of circFBLN2 in the myogenic processes of duck, we conducted experiments involving both the silencing and overexpression of circFBLN2 in DPMs. Our findings indicated that circFBLN2 inhibits DPM proliferation while promoting their differentiation. Conversely, when miR-22-5p was silenced and overexpressed, it exhibited opposing effects by promoting the proliferation of DPMs and inhibiting their differentiation. These results suggest a complex dynamic interplay between circFBLN2 and miR-22-5p in the regulation of DPMs proliferation and differentiation. Additionally, our results revealed that both circFBLN2 and myocyte enhancer factor 2 C (MEF2C) act as sponges for miR-22-5p, as demonstrated by binding predictions and dual-luciferase reporter assays. These results offer novel perspectives on the regulatory pathways underlying the duck embryonic skeletal muscle development, underscoring the pivotal function of circFBLN2 in the regulation of miR-22-5p expression. This research deepens our comprehension of the molecular underpinnings of avian myogenesis, potentially paving the way for more effective approaches to bolster growth and development of livestock.

Introduction

Duck meat is an important source of protein and nutrition in China, significantly contributing to the country's meat consumption (Li et al., 2020; Khalid et al., 2020). Skeletal muscle constitutes a substantial portion of an animal's body, typically ranging from 40 % to 60 % of an adult's total weight (Xu et al., 2023). It is crucial for movement, metabolic regulation, and the maintenance of internal homeostasis (Zhao et al., 2022). The skeletal muscle development is influenced by multiple factors, such as genetic makeup, nutritional status, pathological conditions, and environmental influences (Scanes et al., 1984; Güller and Russell, 2010). During the embryonic phase, myoblasts are crucial for skeletal muscle development, giving rise to myotubes or myofibers through processes like activation, migration, adhesion, membrane remodeling, and nuclear fusion (Lehka and Rędowicz, 2020). In birds, muscle tissue development initiates during embryogenesis, while post-hatching growth involves muscle cell expansion and hypertrophy driven by satellite cell fusion (Allen and Boxhorn, 1989; Buckingham et al., 2003). The growth and development of skeletal muscle are regulated by protein-coding genes and various non-coding RNAs.

Scientific section: Genetics and Genomics

* Corresponding author.
E-mail address: chenbiao@jxau.edu.cn (B. Chen).

https://doi.org/10.1016/j.psj.2025.105063
Received 28 November 2024; Accepted 17 March 2025
Available online 18 March 2025

However, the molecular mechanisms by which different types of RNA regulate the proliferation and differentiation of duck myoblasts remain unclear.

circRNAs, initially considered transcriptional byproducts, are now recognized as non-coding RNAs with a covalently closed loop structure formed via back-splicing of precursor mRNAs (Li et al., 2018; Chen et al., 2021a). In recent years, the identification of circRNAs within eukaryotic transcriptomes has been achieved, and as a result, their functions are increasingly being explored. Numerous researches indicate that circRNAs frequently function as molecular sponges for miRNAs, influencing various biological processes through the competing endogenous RNA (ceRNA) mechanism (Lei et al., 2022). For example, circPTPN4 has been shown to act as a ceRNA by sponging miR-499-3p, regulating *NAMPT* expression to enhance myoblast proliferation, differentiation, and fast-twitch muscle phenotype activation (Cai et al., 2022). The expression levels of circRNAs are notably abundant within the skeletal muscle tissues across a spectrum of species, as indicated by prior research (Li et al., 2021; Hu et al., 2021). Our team sequenced duck breast muscle samples at embryonic days 13 and 19, discovering numerous differentially expressed circRNAs, notably circGAS2-2, which enhances cell cycling and myoblast proliferation (Liu et al., 2023a).

MicroRNAs (miRNAs) are short endogenous RNA molecules, generally ranging from 18 to 25 nucleotides, found widely throughout eukaryotes (Ambros, 2004). They modulate gene expression by targeting mRNA, thus controlling post-transcriptional levels of genes and playing crucial roles in cell proliferation and differentiation (Correia de Sousa et al., 2019). Research has demonstrated that miRNA sequencing reveals a notable presence of conserved miRNAs in duck skeletal muscle across various developmental stages (Gu et al., 2014; Huang et al., 2024). These miRNAs have been implicated in numerous biological processes, including the development of skeletal muscle (Bartel, 2004). For instance, study indicate that miRNA-1 targets *HDAC4* to promote duck myoblast differentiation, while miRNA-133 influences the expression of *SRF* and *TGFBR1* to enhance duck myoblast proliferation (Wu et al., 2019). In addition, miR-301a-3p promotes the proliferation and differentiation of Muscovy duck satellite cells by targeting *ANKRD1* (Huang et al., 2024). Nonetheless, the molecular function of miR-22-5p in ducks skeletal muscle remains unreported.

In previous RNA sequencing of duck primary myoblasts, we discovered a novel circular RNA, circFBLN2, from the second exon of the duck *FBLN2* gene, showing differential expression between the proliferation and differentiation stages (Liu et al., 2023b). We validated the differential expression of circFBLN2 between GM and DM using quantitative real-time PCR (qRT-PCR). Besides, it was also found to be differentially expressed at various stages of development in duck pectoral and leg muscles. Notably, we predicted that circFBLN2 contains potential binding sites for miR-22-5p. Therefore, we hypothesized that circFBLN2 may potentially regulate the development of duck skeletal muscle. In this study, we sought to explore the interaction between circFBLN2 and miR-22-5p, as well as their roles in regulating DPMs proliferation and differentiation. Our results demonstrate that circFBLN2 suppresses proliferation and facilitates differentiation of DPMs by acting as a sponge for miR-22-5p. Conversely, miR-22-5p promotes proliferation while inhibiting differentiation by reducing the expression of myocyte enhancer factor 2C (MEF2C).

Materials and methods

Ethics Statement

A rigorous set of ethical guidelines set forth by Jiangxi Agricultural University and national regulations regarding animal ethics and welfare were followed in this study ([2018]30). All ducks and embryos were treated humanely throughout the research.

Samples Collection

In accordance with previous protocols, a total of 200 hatching eggs from Shan Ma ducks were sourced from the Jiangxi Tianhou Xuanniao Agricultural Technology Co., Ltd. (Nanchang, China). These eggs were incubated under conditions of 37.2°C and relative humidity maintained at 60 ± 10 % (Liu et al., 2023a). Starting from embryonic day 10 (E10) to post-hatch day 1 (P1), duck eggs at E10, E13, E16, E19, E22, and P1 were surface-sterilized. The embryos were then carefully extracted, and their morphology was examined to confirm the appropriate developmental stage. Embryos were rinsed with PBS to remove impurities, and the skin and bones of the legs and pectoral regions were removed. Liver, pectoral muscle, and leg muscle tissue samples were collected, rapidly frozen in liquid nitrogen in 2 mL cryogenic tubes, and stored at −80°C. Genomic DNA was extracted from liver tissues, and the chromodomain helicase DNA-binding protein 1 (CHD1) gene was amplified by PCR to determine the sex of the embryos. Subsequent experiments were conducted using pectoral and leg muscle tissues from embryos of the same sex, with four samples for each period.

Cell Culture and Transfection

An established method was used to isolate DPMs from the breast and leg muscles of 13-day embryonic age (E13) Shan Ma ducks and grow them as described in previous studies (Liu et al., 2011, 2023b). The DPMs were cultured in RPMI 1640 medium (Gibco, Waltham, MA) supplemented with 0.2 % penicillin-streptomycin (Solarbio, Beijing, China) and 10 % fetal bovine serum (Gibco) at 37°C in a 5 % CO_2 atmosphere. Chicken fibroblasts (DF-1) were maintained in DMEM medium (Gibco) supplemented with 10 % fetal bovine serum and 0.2 % penicillin-streptomycin. For transfection assays, various constructs were transiently introduced into the cells using Lipofectamine 3000 (Invitrogen, Carlsbad, CA). The constructs included the pK25ssAAV-circFBLN2 vector, small interfering RNAs (siRNAs), miRNA mimics, and miRNA inhibitors, along with their respective negative controls: pK25ssAAV-ciR vector, siRNA negative control (siRNA NC), mimic negative control (mimic NC), and inhibitor negative control (inhibitor NC).

RNA Exaction, cDNA Synthesis and qRT-PCR

Total RNA was isolated from cultured cells, breast muscle, and leg muscle tissues using Trizol Reagent (TaKaRa, Tokyo, Japan) in accordance with the manufacturer's protocol. RNA quality and concentration were determined using a NanoDrop 2000 spectrophotometer (Thermo Fisher, Waltham, MA). Following RNA extraction, cDNA synthesis was carried out using reagents and conditions as described in our previously published study (Liu et al., 2023b). The relative RNA expression levels were quantified via qRT-PCR performed in a 20 μL reaction volume using 2 × T5 Fast qPCR Mix (Tsingke, Beijing, China), with *GAPDH* and *U6* serving as internal controls for mRNA and miRNA, respectively. All qRT-PCR experiments were conducted on the ABI QuantStudio 5 system (Thermo Fisher), adhering to the reagents and protocols detailed in our earlier publication (Chen et al., 2022). The qRT-PCR reaction data were analyzed using the comparative $2^{-\Delta\Delta Ct}$ method (Livak and Schmittgen, 2001), with all reactions conducted in triplicate. Each group consisted of four biological replicates ($n = 4$).

Primers

Primers for mRNA amplification were designed using the Primer-BLAST tool available on the NCBI website (https://blast.ncbi.nlm.nih.gov/Blast.cgi?PROGRAM=blastn&PAGE_TYPE=BlastSearch&LINK_LOC=blasthome). For circRNA amplification, primers were designed using Oligo 7.0 software. Specific bulge-loop qRT-PCR primers for miRNA detection were provided by Ribobio (Guangzhou, China).

Table 1
Primers for qRT-PCR.

Gene	Primer sequences (5′→3′)	Product size (bp)	Annealing temperature (°C)	Application
CHD1	Z: TGCAGAAGCAATATTACAAGT W: AATTCATTATCATCTGGTGG	250~500	51	PCR
Convergent-circFBLN2	F: ATCAGCTGCCAGTTCATGCT R: GGTGAGTGGTACGGTCGTTT	492	60	validation of circFBLN2
Divergent-circFBLN2	F: TTCAGTGCCACAACCTCTCC R: CACGTCCTCGATGCAGTTGT	412	60	validation of circFBLN2
MEF2C	F: CTACGATGGGAGTGACCGTG R: CTTGACAGAGGGGCTTTCCC	100	60	qRT-PCR
MYOD	F: CGACGGCATGATGGAGTACA R: TGAGAGGCAATCAAGGCTGG	139	60	qRT-PCR
MYOG	F: CCGGACCAGAGGTTTTACGA R: CAAAGCCACCCTGCTTTCG	120	60	qRT-PCR
CCND1	F: ATGCCAACCTCCTCAACGAC R: GCACTTGAAGTAGGACACCGA	86	60	qRT-PCR
CCND2	F: AGTTGACGCGTTTTTCCAGC R: CGGTCGTCGTAGAGCAAGTT	138	60	qRT-PCR
CDK2	F: TCAAGAGCTACCTGTTCCAGC R: CGAAATCGGCCAGCTTGATG	129	60	qRT-PCR
Duck-GAPDH	F: GGTAGTGAAGGCTGCTGCTGATG R: CCACCACACGGTTGCTGTATCC	197	60	qRT-PCR
DF1-GAPDH	F: CAACTTTGGCATTGTGGAGG R: CGCTGGGATGATGTTCTGG	130	60	qRT-PCR

Table 2
RNA oligonucleotides in this study.

Gene	sequences (5′→3′)
circFBLN2-si1	Sense: GGUUACCAGAAGGAUCUAUTT Antisense: AUAGAUCCUUCUGGUAACCTT
circFBLN2-si2	Sense: CCAGAAGGAUCUAUGAGAATT Antisense: UUCUCAUAGAUCCUUCUGGTT
si-NC	Sense: UUCUCCGAACGUGUCACGUTT Antisense: ACGUGACACGUUCGGAGAATT
miR-22-5p mimic	Sense: AGUUCUUCAGUGGCAAGCUUUA Antisense: AAGCUUGCCACUGAAGAACUUU
mimic NC	Sense: UUCUCCGAACGUGUCACGUTT Antisense: ACGUGACACGUUCGGAGAATT
miR-22-5p inhibitor	UAAAGCUUGCCACUGAAGAACU
inhibitor NC	CAGUACUUUUGUGUAGUACAA

Detailed information on all primers utilized in this study is presented in Table 1.

Validation assay of circFBLN2 Existence and Circular Structure

To confirm the presence and loop structure of circFBLN2, convergent and divergent primers were designed based on previous sequencing data (Liu et al., 2023b) and the NCBI reference sequences for *FBLN2* (XM_038185839.1). PCR reactions were conducted using genomic DNA and cDNA derived from DPMs to confirm the junction of circFBLN2. Meanwhile, circFBLN2 was digested with RNase R to confirm its circular form, following the experimental procedures described in previous study (Tian et al., 2023). To assess circFBLN2 expression levels in DPMs, we isolated nuclear and cytoplasmic RNAs using the Cytoplasmic & Nuclear RNA Purification Kit (Norgen Biotek, Thorold, Canada). The isolated RNAs were then used for cDNA synthesis prior to qRT-PCR analysis, with each sample processed in triplicate.

Plasmids Construction and RNA Oligonucleotides Synthesis

Based on previous sequencing data, the circFBLN2 sequence was synthesized by Tsingke and cloned into the pK25ssAAV-ciR vector. For the construction of the pmirGLO dual-luciferase reporter vectors, wild type (circFBLN2-WT, *MEF2C* 3′UTR-WT) and mutant type (circFBLN2-MT, *MEF2C* 3′UTR-MT) sequences from the *MEF2C* 3′UTR and a segment of circFBLN2, both containing the predicted miR-22-5p binding sites, were synthesized. These sequences were inserted into pmirGLO vectors by Tsingke.

GenePharma (Shanghai, China) designed and synthesized siRNAs targeting circFBLN2, along with the miR-22-5p mimic, mimic NC, miR-22-5p inhibitor, and inhibitor NC. Detailed sequences are provided in Table 2.

EdU Assay

After 36-48 h of transfection, both the treated DPMs and NC groups in 24-well plates were exposed to 10 μM 5-Ethynyl-2′-Deoxyuridine (MeilunBio, Dalian, China) at 37 °C for 2 h. Following this incubation, DPMs were fixed, permeabilized, and stained according to the instructions of manufacturer. A fluorescence microscope (TS2R-FL, Nikon, Tokyo, Japan) was used to capture images of EdU-stained cells. ImageJ v1.8.0 software (Schneider et al., 2012) was used to quantify EdU-positive cells. Each group consisted of six biological replicates ($n = 6$).

CCK-8 Assay

At 12-, 24-, 36-, and 48- hours after transfection, 10 μL of CCK-8 working solution (MeilunBio) was added to DPMs plated in 96-well plates. After a 2-hour incubation at 37°C, absorbance at 450 nm was measured using a Fluorescence/Multi-Detection Microplate Reader (Biotek, Winooski, VT). Each group consisted of six biological replicates ($n = 6$).

Immunofluorescence

For immunofluorescence analysis, DPMs were plated in 24-well plates and transfected at approximately 80 % confluence. 72 h post-transfection, DPMs were fixed, permeabilized, blocked, incubated with primary antibodies, stained with secondary antibodies, and counter-stained for nuclei following the experimental procedures described in previous studies (Sun et al., 2022). The anti-MYHC antibody (MF20, DSHB, Iowa, IA, 3 μg/mL) was used as the primary antibody, while a fluorochrome-conjugated secondary antibody (FITC/Cy3, A0568/A0521, Beyotime, Shanghai, China; 1:500) was employed for detection. DAPI (Servicebio, Wuhan, China) was used for nuclear staining. Finally, the images from the fluorescence microscope (TS2R-FL, Nikon) were captured randomly. The stained myotube area was quantified using ImageJ v1.8.0 software (Schneider et al., 2012)

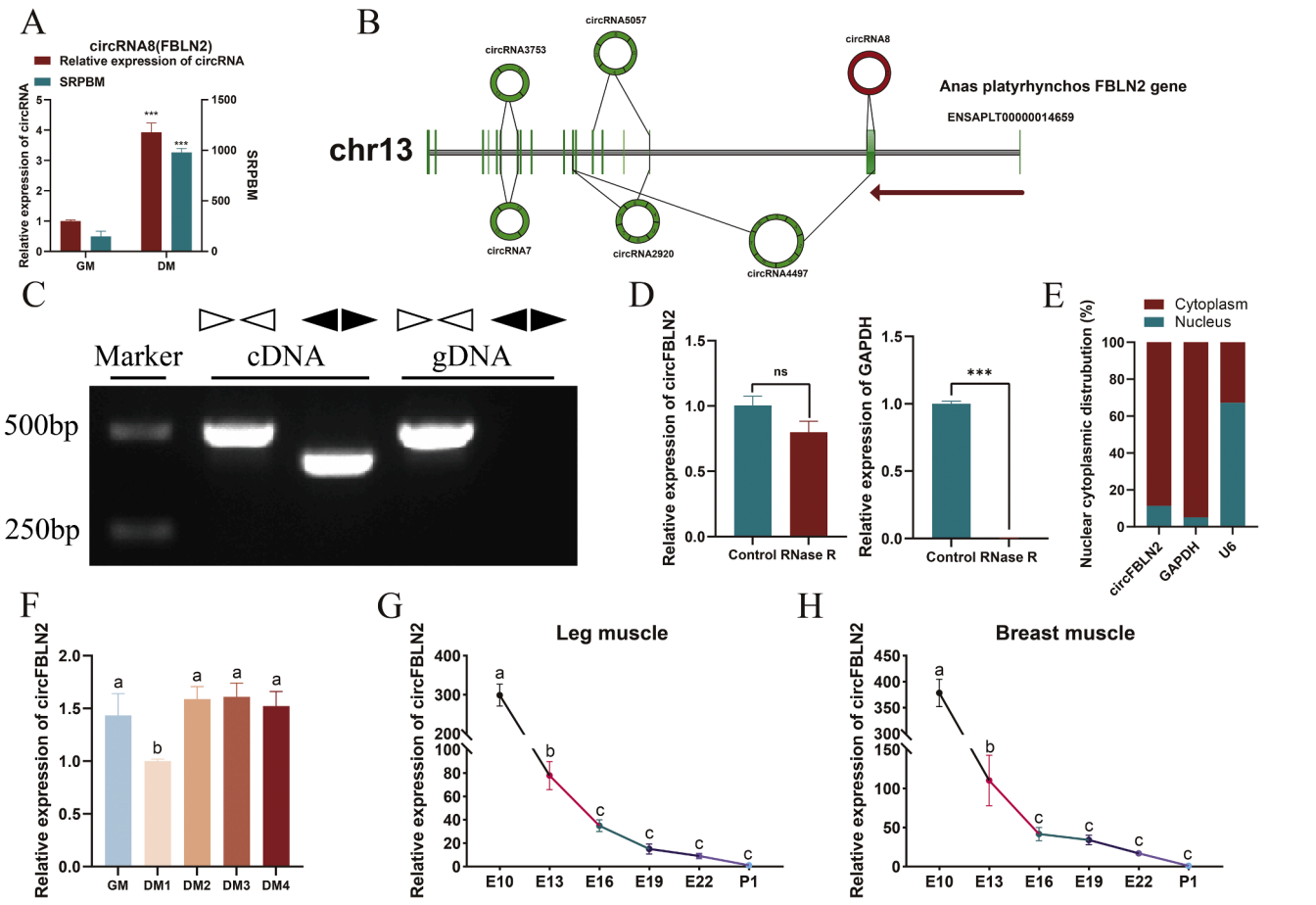

Figure 1. Experimental Validation and Temporal Expression Analysis of circFBLN2. (A) qRT-PCR validation of circFBLN2. SRPBM: spliced reads per billion mapping. (B) The genomic structure of *FBLN2* and the distribution of its circular transcripts. (C) The identification of circFBLN2 was conducted using PCR with convergent (white triangles) and divergent primers (black triangles), with cDNA and gDNA as templates. (D) Verification of circFBLN2 loop presence after RNase R digestion. (E) Subcellular distribution of circFBLN2 in nuclear and cytoplasmic fractions of DPMs. (F) circFBLN2 expression levels during DPM proliferation and differentiation. (G, H) Temporal expression patterns of circFBLN2 in duck embryonic leg muscle and breast muscle at various developmental stages. Data are preferred as mean ± SEM. Distinct letters indicate significant differences between groups ($P < 0.05$). Significance is marked as $^{*}P < 0.05$, $^{**}P < 0.01$, and $^{***}P < 0.001$.

and expressed as a percentage of the total image area occupied by myotubes. Each group consisted of six biological replicates ($n = 6$).

Western Blotting

Western blotting was carried out to assess protein expression levels. DPMs were cultured in 6-well plates, and after 72 h of transfection, total proteins of DPMs were abstracted with RIPA buffer (Beyotime) supplemented with PMSF protease inhibitor (Solarbio) and were determined using a BCA Protein Quantification Kit (Vazyme, Nanjing, China). Total proteins of DPMs were resolved using 10 % SDS-PAGE (Beyotime) and transferred onto polyvinylidene fluoride (PVDF) membranes (0.45 μm, Monad, Suzhou, China). The PVDF membranes were probed with with primary antibodies, including anti-MYHC (MF20, DSHB, 0.3 μg/mL) and anti-GAPDH (60004-1-lg, Proteintech, Wuhan, China; 1:30000), followed by goat anti-mouse IgG (L3032, Signalway Antibody, Greenbelt, MD, 1:30000) as the secondary antibody. Signals were visualized with ECL chemiluminescence solution (Share-bio, Shanghai, China) and captured using the Amersham Imager 680 (General Electric, Fairfield, CT). Band intensities were quantified using ImageJ v1.8.0 software (Schneider et al., 2012). Each group consisted of three biological replicates ($n = 3$).

Prediction of Binding Interactions and Dual-Luciferase Reporter Analysis

Based on the previous sequencing data (Liu et al., 2023b), we used TargetScan v5.0 (Nam et al., 2014) (with a score threshold of ≥50) and miRanda v3.3a (Betel et al., 2010) (with an energy threshold of <−10) to predict the target genes of miR-22-5p. To further investigate potential interactions between miR-22-5p and target genes, we employed RNAhybrid v2.2.3 software (https://bibiserv.cebitec.uni-bielefeld.de/rnahybrid/) (Krüger and Rehmsmeier, 2006). DF-1 cells were plated in 96-well plates and co-transfected with pmirGLO-WT (circFBLN2-WT, MEF2C 3′UTR-WT) or pmirGLO-MT (circFBLN2-MT, MEF2C 3′UTR-MT) along with miR-22-5p mimic or mimic NC. After 48 h, luminescence was assessed using the Dual-GLO Luciferase Assay System Kit (Promega, Madison, WI) and a Biotek Fluorescence/Multi-Detection Microplate Reader, following the manufacturer's protocol. Each group comprises a minimum of six biological replicates ($n \geq 6$).

Statistical Analysis

Results are presented as means ± SEM. Statistical significance between two groups was evaluated with a two-tailed Student's t-test, while one-way ANOVA was used for multi-group comparisons, performed in SPSS v26.0 software. Significance thresholds were set as $^{*}P < 0.05$, $^{**}P < 0.01$, and $^{***}P < 0.001$, with the letters a, b, and c denoting $P < 0.05$.

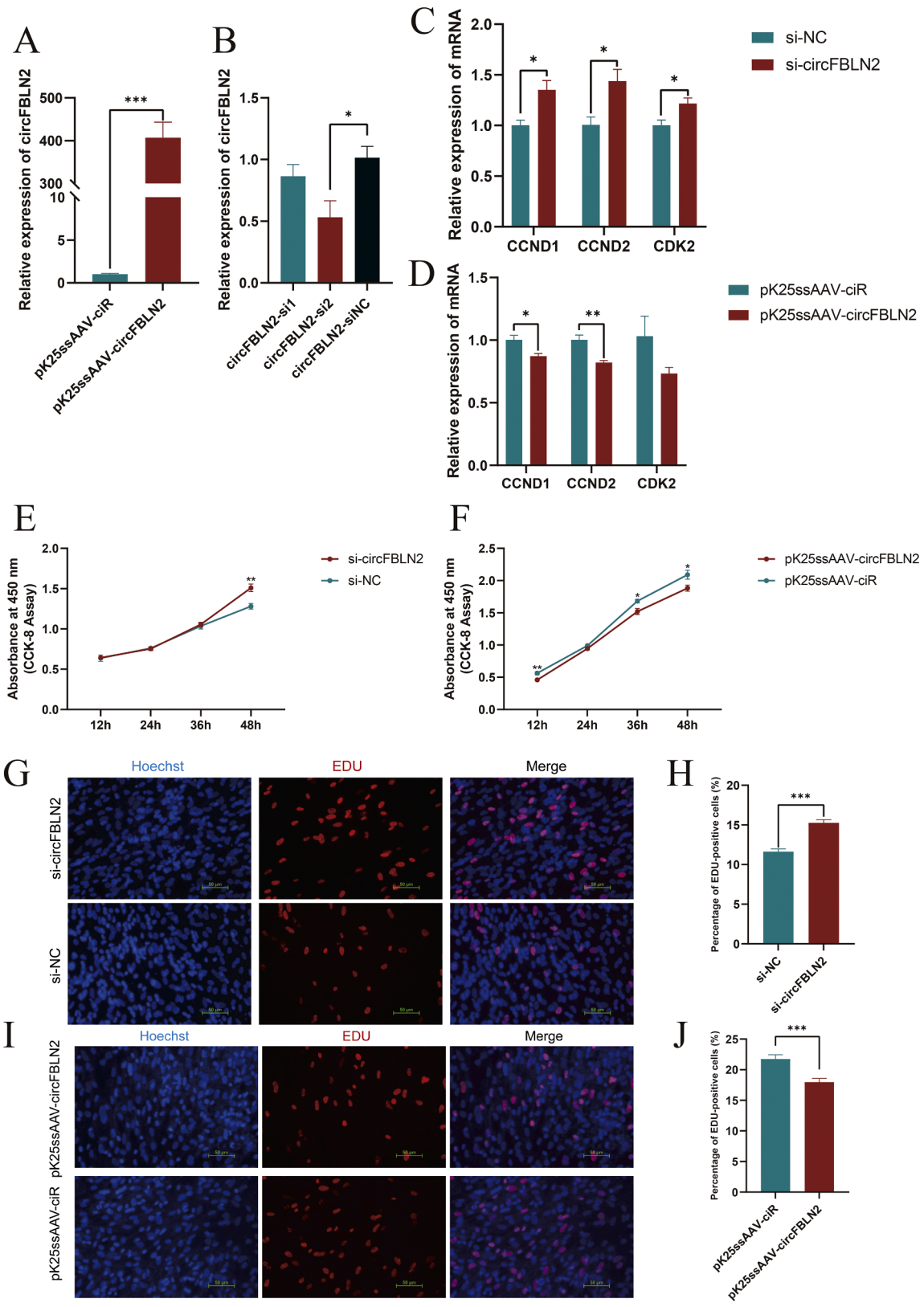

Figure 2. Impact of circFBLN2 on DPMs proliferation. (A, B) Transfection efficiency of the circFBLN2 overexpression vector and two circFBLN2 siRNAs in DPMs. (C, D) The mRNA levels of proliferation marker genes after circFBLN2 interference and overexpression. (E, F) Effect of circFBLN2 interference and overexpression on cell viability as evaluated by the CCK-8 assay. (G, I) EdU assays performed following transfection of DPMs with the circFBLN2 siRNA and overexpression vector. EdU (red) fluorescence marks proliferating cells, while Hoechst (blue) fluorescence labels nuclei. (H, J) This quantification was done for the proportion of EdU-positive cells with inhibition and overexpression of circFBLN2. Data are presented as mean ± SEM. $^{*}P < 0.05$; $^{**}P < 0.01$; $^{***}P < 0.001$.

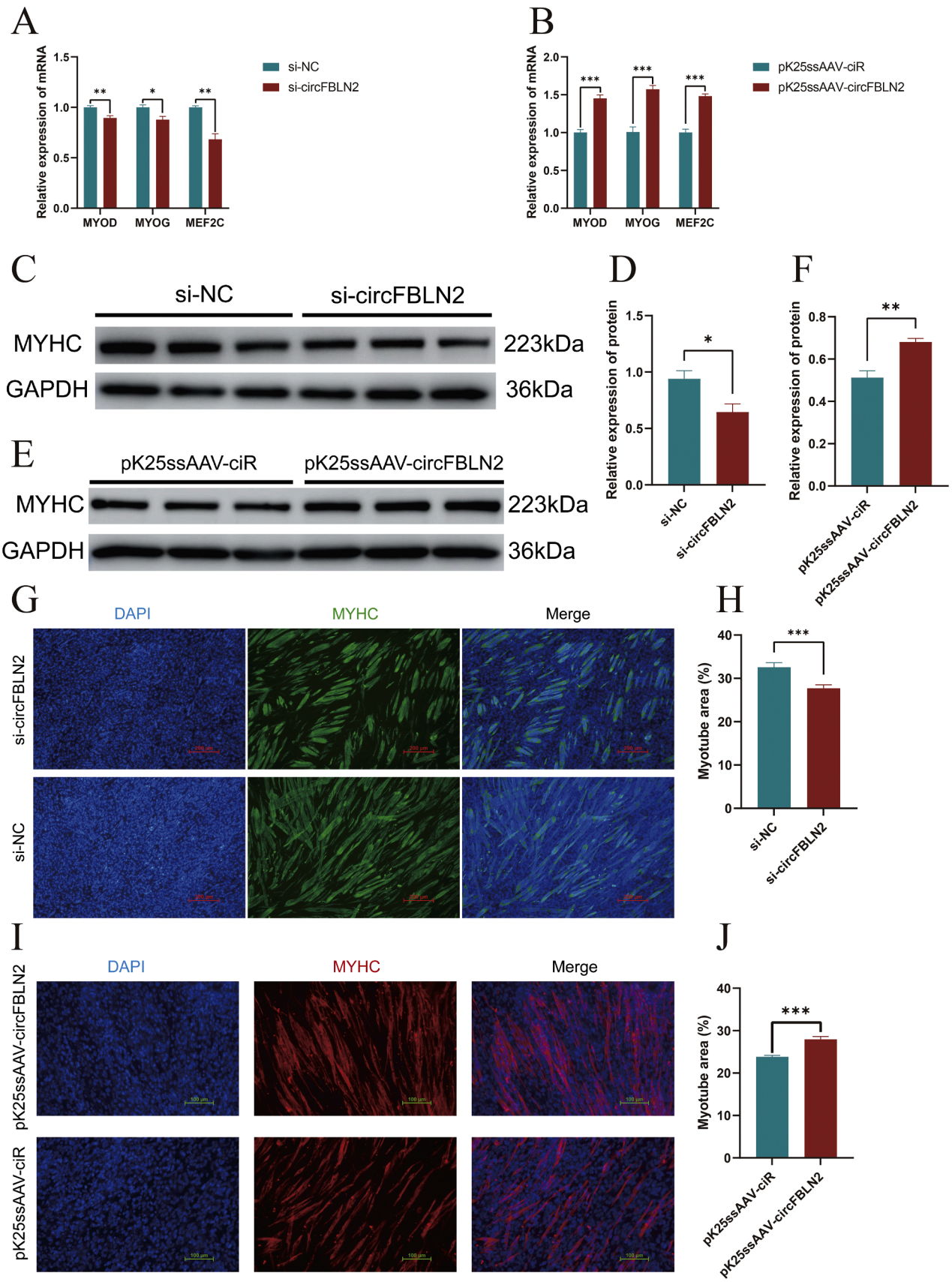

Figure 3. Impact of circFBLN2 on DPMs differentiation. (A, B) The mRNA levels of differentiation marker genes after circFBLN2 interference and overexpression. (C, E) The MYHC protein expression after transfection with circFBLN2 siRNA and overexpression vector. (D, F) Quantified levels of MYHC protein after circFBLN2 interference and overexpression. (G, I) Fluorescence microscopy images after transfection with circFBLN2 siRNA and overexpression vector. (H, J) Statistics of myotube area of the fluorescence microscopy images. Data are shown as mean ± SEM. $^{*}P < 0.05$; $^{**}P < 0.01$; $^{***}P < 0.001$.

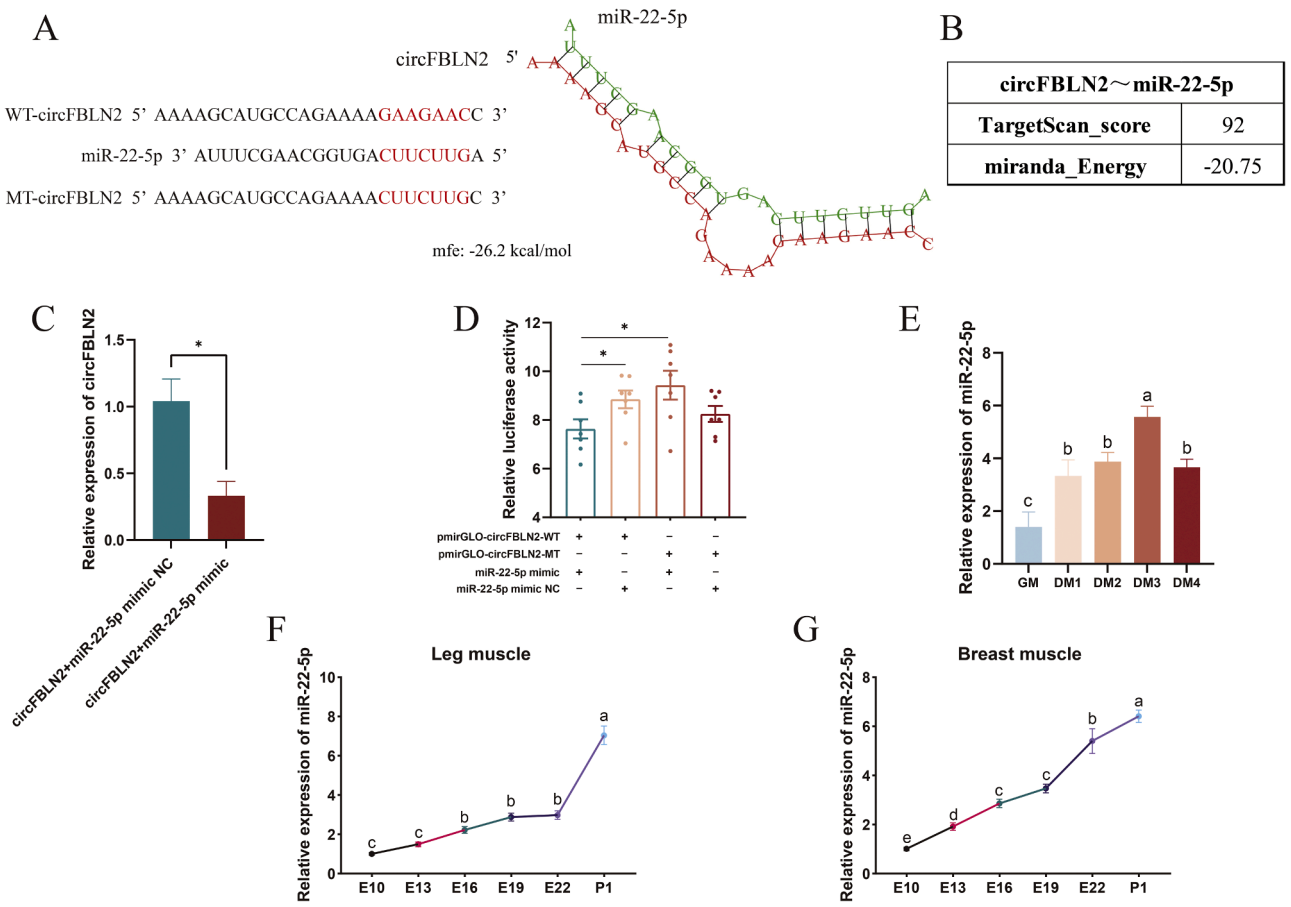

Figure 4. Validation of the interaction between circFBLN2and miR-22-5p. (A) Targeted binding prediction of miR-22-5p and circFBLN2 using from RNAhybrid v2.2.3 software. (B) Predicted interaction outcomes from miRanda v3.3a and TargetScan v5.0 software. (C) Measurement of circFBLN2 expression levels following co-transfection with pK25ssAAV-circFBLN2 and miR-22-5p mimic (or NC). (D) Dual luciferase reporter assay results of miR-22-5p targeting circFBLN2. (E) Changes in relative expression of miR-22-5p during the DPMs proliferation and differentiation. (F, G) Spatial and temporal expression patterns of miR-22-5p in duck embryonic leg and breast muscles at various developmental stages. Data are preferred as means ± SEM. Distinct letters indicate significant differences between groups ($P < 0.05$). Significance is marked as $^*P < 0.05$.

Results

Experimental Validation and Temporal Expression Analysis of circFBLN2

Building on our previous sequencing findings, we observed that circFBLN2 was dramatically upregulated in differentiated DPMs (DM), a result further confirmed by qRT-PCR ($P < 0.001$) (Fig. 1A). Sequencing data indicated that six circRNAs were originated from the *FBLN2* gene. The genomic architecture of the duck *FBLN2* gene, along with the regions from which all circular *FBLN2* RNAs originated, is illustrated in Fig. 1B. Notably, circFBLN2 (labeled as circRNA8 in Fig. 1B) uniquely emerged from the second exon of the *FBLN2* gene located on chromosome 13, distinguishing it as the sole exonic circular RNA. To verify the sequence and junction of circFBLN2, PCR was performed on genomic DNA (gDNA) and complementary DNA (cDNA) using convergent primers and divergent primers. Electrophoresis revealed expected products for convergent primers in both templates, while divergent primers yielded no amplification from gDNA (Fig. 1C). Additionally, treatment with RNase R corroborated the existence of circFBLN2, as qRT-PCR indicated minimal impact on circFBLN2 levels, while the *GAPDH* expression levels, utilized as a linear RNA control, substantially decreased (Fig. 1D). Subcellular fractionation studies revealed that circFBLN2 predominantly localized in the cytoplasm (Fig. 1E).

To thoroughly assess the temporal expression patterns of circFBLN2 during duck muscle development, we analyzed its expression across different stages of DPM differentiation and in pectoral and leg muscle tissues of duck embryos at various embryonic ages, applying qRT-PCR. Our findings demonstrated that circFBLN2 expression fluctuated in accordance with the proliferation and differentiation phases of DPMs, exhibiting a notable initial decline, followed by an increase, and remaining at a similar level from DM2 to DM4 (Fig. 1F). Furthermore, circFBLN2 expression varied with the developmental timeline of duck embryos, showing a notable decline in both leg and pectoral muscles, remaining at a low level from the E16 to P1 stages (Fig. 1G, H). Temporal expression analysis indicated that circFBLN2 could be vital for the development of duck muscle.

circFBLN2 Represses DPMs Proliferation

To investigate how circFBLN2 influences DPM proliferation, we synthesized small interference RNAs targeting circFBLN2 and constructed an overexpression vector for circFBLN2. We transfected 1000 ng of pK25ssAAV-circFBLN2 and 1000 ng of pK25ssAAV-ciR into DPMs in each well of a 12-well plate. qRT-PCR analysis revealed a substantially elevated expression of circFBLN2 in the pK25ssAAV-circFBLN2 group compared to the pK25ssAAV-ciR group ($P < 0.001$) (Fig. 2A). Similarly, we transfected interference RNAs, namely circFBLN2-si1 and circFBLN2-si2 into DPMs. The qRT-PCR results demonstrated that circFBLN2-si2 exhibited a striking interference effect ($P < 0.05$) (Fig. 2B). Of the two siRNAs tested, circFBLN2-si2 showed superior interference efficiency and was selected for subsequent experiments, where it is referred to as si-circFBLN2. In the proliferation experiments,

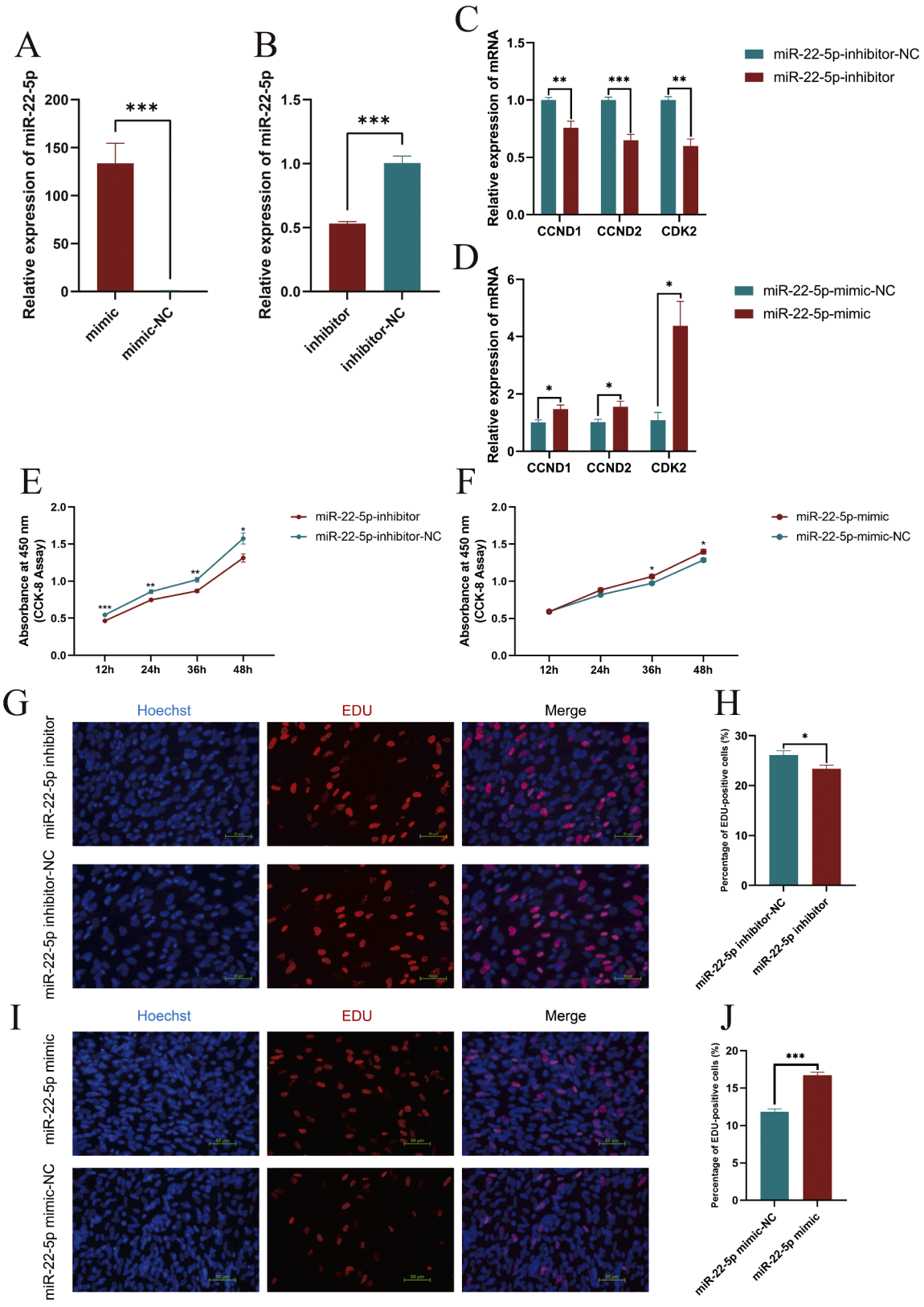

Figure 5. Influence of miR-22-5p on DPM proliferation. (A, B) Efficiency of miR-22-5p mimic and inhibitor transfection. (C, D) Impact of miR-22-5p knockdown and overexpression on proliferation marker gene expression. (E, F) Influence of miR-22-5p interference and overexpression on cell viability as evaluated by the CCK-8 assay. (G, I) EdU assays performed following transfection of DPMs with the miR-22-5p inhibitor and mimic. EdU (red) fluorescence marks proliferating cells, while Hoechst (blue) fluorescence labels nuclei. (H, J) The quantification of the proportion of EdU-positive cells with inhibition and overexpression of miR-22-5p. Data are represented mean ± SEM. $^{*}P < 0.05$; $^{**}P < 0.01$; $^{***}P < 0.001$.

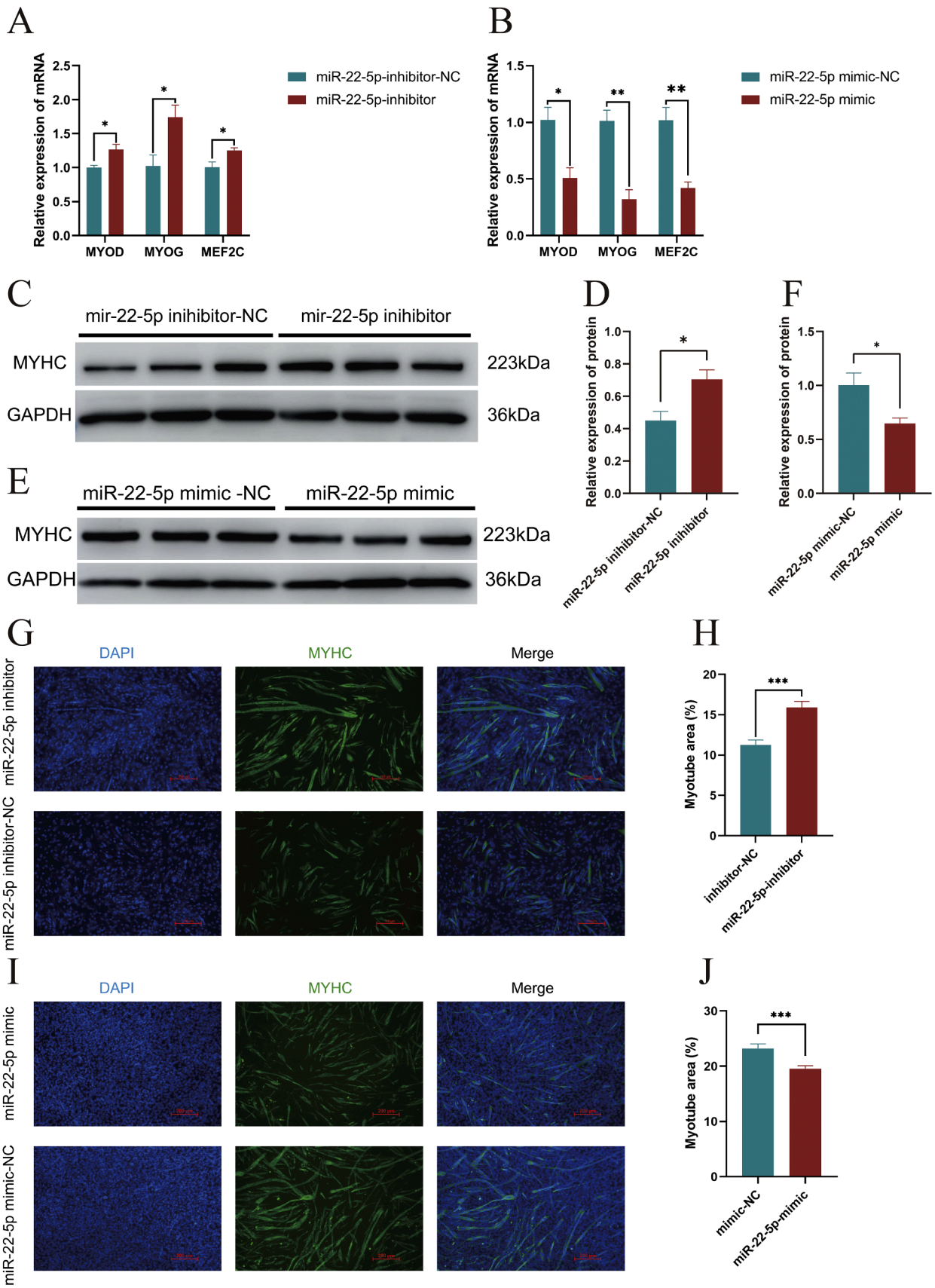

Figure 6. The role of miR-22-5p in DPM differentiation. (A, B) Impact of miR-22-5p interference and overexpression on differentiation marker genes. (C, E) The MYHC protein expression following transfection with miR-22-5p inhibitor and mimic. (D, F) Quantification levels of MYHC protein post-transfection with miR-22-5p inhibitor and mimic. (G, I) Fluorescence microscopy images of DPMs transfected with miR-22-5p inhibitor and mimic. (H, J) Measurement of myotube area after miR-22-5p was silenced and overexpression. Data are represented mean ± SEM. * $P < 0.05$; ** $P < 0.01$; *** $P < 0.001$.

qRT-PCR was employed to assess the expression changes of key proliferation genes, including cyclin D1 (CCND1), cyclin D2 (CCND2), and cyclin-dependent kinase 2 (CDK2), in DPMs. The results presented that following siRNA transfection, the levels of the *CCND1, CCND2*, and *CDK2* expression were prominently elevated ($P < 0.05$) (Fig. 2C). Conversely, transfection with pK25ssAAV-circFBLN2 led to a noticeable reduction in *CCND1* and *CCND2* expression levels ($P < 0.05$), along with a noticeable downward trend in *CDK2* expression (Fig. 2D). The CCK-8 assay showed no obvious changes in absorbance at 450 nm in DPMs at 12-, 24-, or 36- hours after circFBLN2 siRNA transfection ($P > 0.05$), but a marked increase was observed at 48 h ($P < 0.01$) (Fig. 2E). In contradistinction, transfection with pK25ssAAV-circFBLN2 saliently reduced absorbance at 450 nm at 12-, 36-, and 48-hours post-transfection ($P < 0.05$ or $P < 0.01$) (Fig. 2F). Meanwhile, EdU staining was utilized to further evaluate cell proliferation rates. EdU staining revealed a pronounced rise in the proportion of cells in the proliferation phase following circFBLN2 siRNA transfection compared to the control group ($P < 0.001$) (Fig. 2G, H). In contrast, transfection with the pK25ssAAV-circFBLN2 dramatically decreased the proportion of proliferating cells ($P < 0.001$) (Fig. 2I, J). In summary, circFBLN2 plays a role in inhibiting the proliferation of DPMs.

circFBLN2 Enhances DPMs Differentiation

To investigate circFBLN2's role in DPM differentiation, DPMs were transfected with circFBLN2 siRNA or the overexpression vector pK25ssAAV-circFBLN2. Changes in the expression of differentiation marker genes myogenic differentiation (MYOD), myogenin (MYOG), and *MEF2C* were assessed via qRT-PCR. Transfection with circFBLN2 siRNA saliently reduced *MYOD, MYOG*, and *MEF2C* expression ($P < 0.05$ or $P < 0.01$) (Fig. 3A). Reciprocally, transfection with the overexpression vector pK25ssAAV-circFBLN2 resulted in a pronounced upregulation of these genes ($P < 0.001$) (Fig. 3B). Meanwhile, the protein expression of myosin heavy chain (MYHC) was evaluated, revealing that circFBLN2 siRNA prominently inhibited MYHC levels ($P < 0.05$) (Fig. 3C, D), whereas pK25ssAAV-circFBLN2 sensibly promoted MYHC protein expression ($P < 0.01$) (Fig. 3E, F). Furthermore, immunofluorescence analysis demonstrated that transfection with circFBLN2 siRNA markedly reduced the area of myotube formation ($P < 0.001$) (Fig. 3G, H), while transfection with pK25ssAAV-circFBLN2 prominently increased the area of myotube formation ($P < 0.001$) (Fig. 3I, J). In summary, circFBLN2 promotes the DPMs differentiation.

circFBLN2 Acts as a Sponger for miR-22-5p

RNAhybrid v2.2.3 software predicted potential binding sites between circFBLN2 and miR-22-5p, revealing a stable match with the seed sequence of miR-22-5p within circFBLN2 (Fig. 4A). Predictions from miRanda v3.3a and TargetScan v5.0 identified a strong association between circFBLN2 and miR-22-5p, with a miRanda binding energy of −20.75 and a TargetScan score of 92 (Fig. 4B). These prediction results suggested a strong potential for targeted binding between circFBLN2 and miR-22-5p. To thoroughly clarify the relationship between circFBLN2 and miR-22-5p, we performed co-transfection experiments in DF-1 cells with the pK25ssAAV-circFBLN2 vector and either a miR-22-5p mimic or a negative control (mimic NC). The results showed a noticeable downregulation in circFBLN2 expression levels in the miR-22-5p mimic group compared to the mimic NC group (Fig. 4C). Concurrently, the dual-luciferase reporter assay results displayed a remarkable decrease in fluorescence activity in the WT-circFBLN2 + miR-22-5p mimic group compared to the MT-circFBLN2 + miR-22-5p mimic group ($P < 0.05$) (Fig. 4D). These results indicate a target binding relationship between miR-22-5p and circFBLN2.

Moreover, the expression profile of miR-22-5p exhibited an inverse relationship with that of circFBLN2 throughout various stages of DPM differentiation and in the pectoral and leg muscles of duck embryos. Specifically, miR-22-5p expression initially rose before declining, reaching its peak during the DM3 stage of DPM differentiation (Fig. 4E). Interestingly, miR-22-5p showed a pronounced upward trend in both leg and pectoral muscles, achieving its highest expression level at the P1 stage (Fig. 4F, G).

miR-22-5p Promotes DPMs Proliferation

To examine miR-22-5p's impact on DPM proliferation, DPMs were transfected with 150 nM of either a miR-22-5p mimic or miR-22-5p inhibitor to assess its overexpression and inhibitory effects. The miR-22-5p mimic and inhibitor exhibited the expected effects relative to their respective negative controls (mimic NC and inhibitor NC) (Fig. 5A, B). In the proliferation experiments, qRT-PCR was employed to analyze the expression levels of the proliferation markers *CCND1, CCND2*, and *CDK2* in DPMs. The results indicated that transfection with the miR-22-5p inhibitor sensibly restrained the proliferation marker genes ($P < 0.01$ or $P < 0.001$) (Fig. 5C). Conversely, the miR-22-5p mimic prominently upregulated the expression of the same genes ($P < 0.05$) (Fig. 5D).

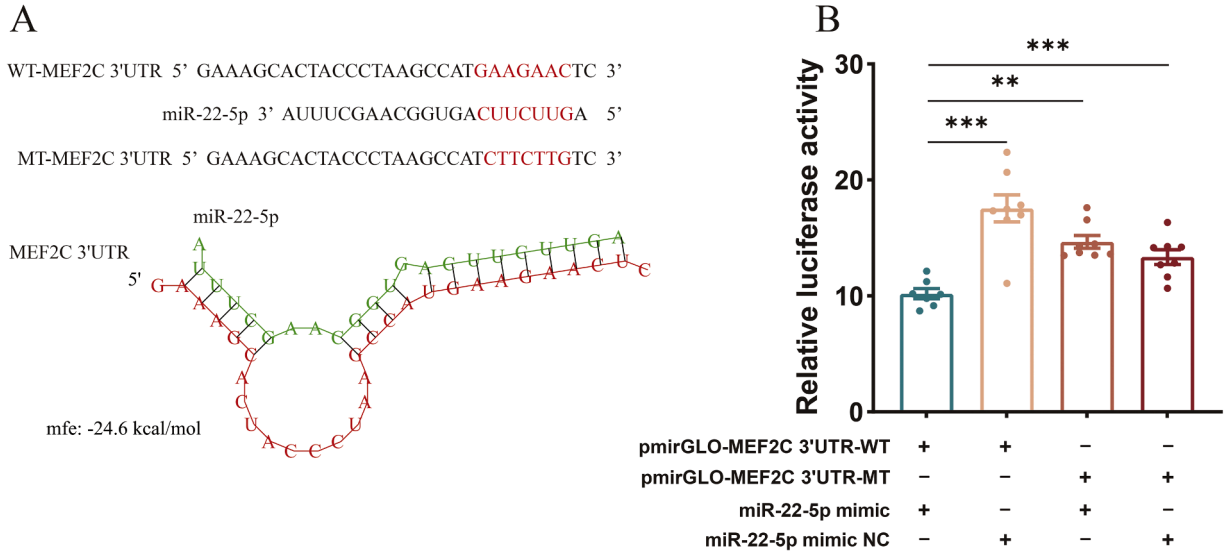

Figure 7. Validation of the interaction between miR-22-5p and *MEF2C*. (A) Targeted binding prediction of miR-22-5p and *MEF2C* using from RNAhybrid v2.2.3 software. (B) Dual-luciferase assay confirming miR-22-5p's regulation of *MEF2C*.

Simultaneously, Cell viability, assessed via the CCK-8 assay, showed a marked reduction in absorbance at 450 nm for DPMs at 12-, 24-, 36-, and 48-hours following transfection with the miR-22-5p inhibitor ($P < 0.05$, $P < 0.01$, or $P < 0.001$) (Fig. 5E). In contrast, the miR-22-5p mimic showed no obvious impact on absorbance at 12- and 24- hours ($P > 0.05$), but a notable increase was observed at 36- and 48- hours ($P < 0.05$) (Fig. 5F). The CCK-8 assay findings suggested that miR-22-5p can promote DPMs proliferation. Correspondingly, EdU assay results demonstrated that inhibiting miR-22-5p through transfection significantly reduced the proportion of proliferating cells compared to the control group ($P < 0.05$) (Fig. 5G, H). Alternatively, introducing the miR-22-5p mimic notably increased the proliferation rate ($P < 0.001$) (Fig. 5I, J). The EdU assay results further corroborate that miR-22-5p can enhance DPMs proliferation.

miR-22-5p Inhibits DPMs Differentiation

To assess how miR-22-5p influences DPMs differentiation, we transfected DPMs with a miR-22-5p inhibitor and mimic and analyzed the expression of differentiation markers *MYOD, MYOG*, and *MEF2C* using qRT-PCR. The results evinced that miR-22-5p inhibitor transfection remarkably augmented the expression of *MYOD, MYOG*, and *MEF2C* ($P < 0.05$) (Fig. 6A). Instead, miR-22-5p mimic transfection notably reduced the expression of these differentiation marker genes ($P < 0.05$ or $P < 0.01$) (Fig. 6B). Meanwhile, the protein expression of MYHC was evaluated, finding that the miR-22-5p inhibitor meaningfully promoted MYHC levels ($P < 0.05$) (Fig. 6C, D), whereas the miR-22-5p mimic significantly inhibited MYHC levels ($P < 0.05$) (Fig. 6E, F). Correspondingly, immunofluorescence analysis demonstrated that miR-22-5p inhibitor markedly increased the area of myotube formation ($P < 0.001$) (Fig. 6G, H), while the miR-22-5p mimic considerably reduced the area of myotube formation ($P < 0.001$) (Fig. 6I, J). In summary, these findings demonstrate that miR-22-5p inhibits the DPMs differentiation.

MEF2C Serves as a Direct Target of miR-22-5p

To explore the role of miR-22-5p in DPM differentiation, we focused on identifying differentiation marker genes targeted by miR-22-5p. The prediction results obtained using TargetScan v5.0 and miRanda v3.3a, which include genes related to skeletal muscle such as *MYL9, GRB2*, and *CLCN1*, are presented in Supplementary Table S1. Additionally, using RNAhybrid v2.2.3 software, we identified conserved miR-22-5p target sites within the 3′UTR region of *MEF2C* (Fig. 7A). Additionally, previous results showed a notable downregulation in MEF2C mRNA levels in the miR-22-5p overexpression group (Fig. 6A). To confirm the association between miR-22-5p and *MEF2C*, we constructed a pmirGLO dual-luciferase miRNA target expression vector by incorporating sequences containing either the wild-type or mutated binding site. These vectors were co-transfected with either a miR-22-5p mimic or mimic NC. The dual-luciferase reporter assay showed significantly reduced luminescence activity in groups with wild-type plasmids and miR-22-5p mimic, compared to controls containing mutated reporters with the mimic or both plasmid types with mimic NC (Fig. 7B). In aggregate, the results imply that *MEF2C* serves as an absorbent for miR-22-5p at the molecular level.

Discussion

Identifying new factors and mechanisms that govern skeletal muscle physiology and development is vital for improving animal health and enhancing the productivity of livestock and poultry (Velleman, 2019; Mo et al., 2023). In this study, we identified a novel circular RNA (circFBLN2) that exhibits elevated expression during the differentiation stage (DM) of DPMs compared to the proliferation stage (GM), based on our prior whole-transcriptome RNA sequencing data. Furthermore, we observed that circFBLN2 was consistently expressed at high levels in both leg and pectoral muscles at embryonic day 10 (E10). However, its abundance memorably decreased in these muscle tissues as embryonic development progressed. This study focused on examining circFBLN2's role in duck myoblast proliferation and differentiation, as well as the mechanisms through which it influences skeletal muscle development.

Recent advancements in high-throughput transcriptome sequencing technologies and bioinformatics have enabled the widespread identification of numerous circRNAs across different species (Szabo and Salzman, 2016). As research in this area evolves, it has become increasingly clear that circRNAs are integral to numerous biological processes, exerting diverse regulatory effects (Ballarino et al., 2016). Specifically, circRNAs function as molecular sponges for miRNAs, encode peptides, interact with RNA-binding proteins, and participate in transcriptional regulation (Liu and Chen, 2022). For instance, Wu et al. found that circLRRFIP1 interacts with the miR-15 family, triggering the AKT3-mTOR/p70S6 K pathway and promoting chicken myoblast growth and differentiation (Wu et al., 2023). circRNAs can also encode peptides, as shown by Lin et al., who discovered that circKANSL1 L in pig muscle encodes a protein interacting with Akt, boosting FoxO3 activity to aid muscle development (Lin et al., 2024). In cattle, circMYBPC1 promotes myoblast differentiation by binding to miR-23a and interacting with *MYHC* to support muscle regeneration (Chen et al., 2021b). Our previous transcriptome analyses showed significant changes in circRNA expression during duck skeletal muscle development and DPM differentiation, underscoring their crucial role in regulating this process (Liu et al., 2023a; b). miRNAs are ubiquitously present in cells and tissues, serving as key regulators of post-transcriptional gene expression in biological development (Rogg et al., 2018; Treiber et al., 2019; Yasmeen et al., 2019). Specific miRNAs, including the miR-1, miR-133, miR-206, and miR-208 families, are prominently expressed in skeletal muscle, regulating gene expression and influencing key processes such as myoblast proliferation, differentiation, muscle regeneration, and fiber type transformation (Chen et al., 2006; van Rooij et al., 2008; Siracusa et al., 2018). Additionally, miRNAs like miR-30a-3p and miR-22-3p, though not specific to skeletal muscle, aid in its growth and development (Wang et al., 2022; Li et al., 2022). For instance, miR-142a-3p modulates muscle differentiation and regeneration by targeting *MEF2A* expression during skeletal muscle development (Gu et al., 2023). Equally, exosome-derived miRNAs significantly impact skeletal muscle function, such as miR-29, which reduces muscle atrophy in mice by inhibiting *YY1* and TGF-β pathway proteins (Wang et al., 2019). Moreover, exosomal miR-27a from adipocytes can inhibit *PPARγ*, thereby inducing insulin resistance in skeletal muscle (Yu Y et al., 2018).

The primary regulatory factors of the cell cycle include cyclins, cyclin-dependent kinases (CDKs), and CDKs inhibitors (CDKIs) (Hydbring et al., 2016; Zhang et al., 2021). In eukaryotes, its progression depends on cyclin-CDK complex formation (Malumbres and Barbacid, 2009). In addition, studies also indicated that *CCND1, CCND2*, and *CDK2* are key components in maintaining cell cycle control (Helsten et al., 2016; Wood and Endicott, 2018). *MYOD* and *MYOG*, key myogenic regulatory factors (MRFs), drive skeletal muscle cell differentiation during both embryonic and postnatal myogenesis, facilitating muscle growth and development (Zammit, 2017; Adhikari et al., 2021). *MEF2C*, a member of the MEF2 family, is essential for myogenesis and myoblast differentiation (Liu et al., 2014). MYHC is an important component of myosin, involved in the formation of thick filaments in myofibrils, and serves as a marker for myoblast differentiation (Tajsharghi and Oldfors, 2013). In this present study, circFBLN2 was shown to suppress DPM proliferation by downregulating proliferation marker genes (*CCND1, CCND2, CDK2*), as confirmed through CCK-8 and EdU assays. Moreover, increased mRNA levels of differentiation markers (*MYOD, MYOG, MEF2C*), elevated MYHC protein expression, and the relative area of MYHC in the myotubes confirmed that circFBLN2 could facilitate DPMs differentiation. Reciprocally, we found that miR-22-5p

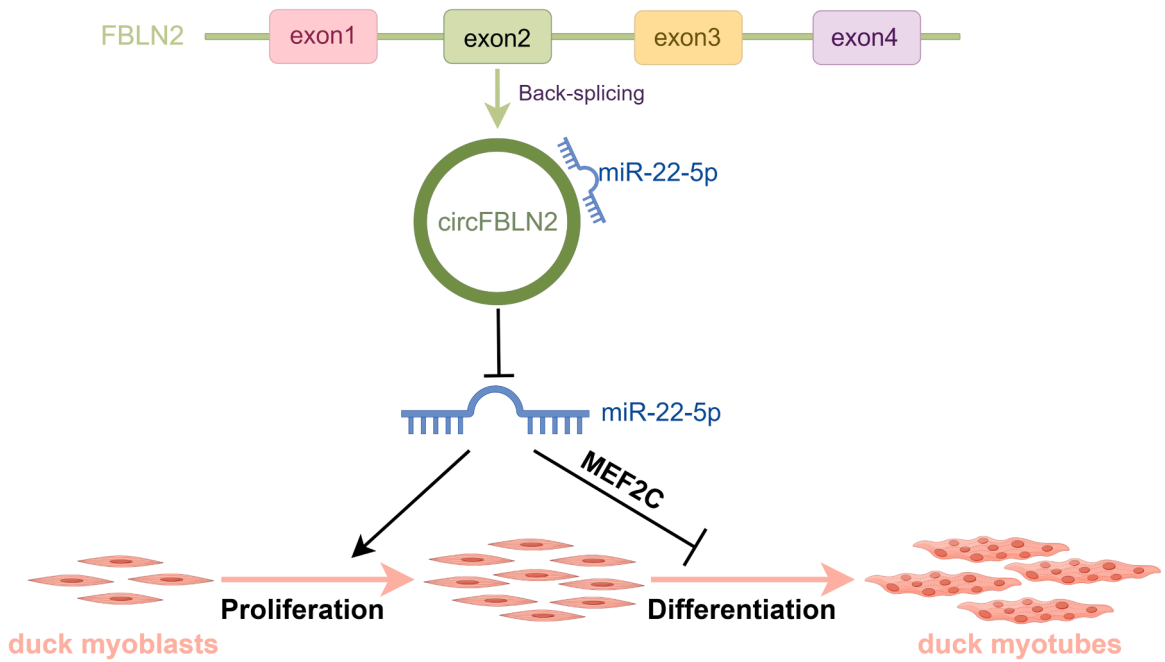

Figure 8. The regulatory role model of circFBLN2 in DPMs proliferation and differentiation. circFBLN2 represses DPMs proliferation and promotes DPMs differentiation by sponging miR-22-5p. In contrast, miR-22-5p enhances proliferation and suppresses differentiation by downregulating *MEF2C* expression. This figure was generated using Figdraw.

promoted DPMs proliferation while inhibiting their differentiation. Overall, circFBLN2 and miR-22-5p were identified as key regulators of DPMs proliferation and differentiation, contributing to duck skeletal muscle development.

Recent studies have demonstrated that miR-22-5p is implicated in a variety of biological processes across multiple species. Notably, research has shown that miR-22-5p targets *EZH2* to inhibit spermatogonial stem cell proliferation and *LEF1* to suppress hair follicle stem cell growth (Yan et al., 2019; Lv et al., 2022). In contrast, our findings indicate that miR-22-5p promotes proliferation in duck myoblasts. Similarly, miR-22-5p has been observed to inhibit both the proliferation and differentiation of porcine skeletal muscle satellite cells, suggesting that its function may be specific to certain species or tissue types (Shi et al., 2024). Further comparative studies employing both avian and mammalian models are necessary to elucidate these regulatory discrepancies.

Circular RNA with miRNA response elements (MREs) often function as miRNA sponges, employing ceRNA mechanisms to modulate post-transcriptional gene expression and influence biological processes (Hansen et al., 2013). After miRNA binds with RISC, it recognizes and inhibits the translation of target RNA (Bartel, 2004). While circFBLN2 has not been extensively studied in other models, similar circRNAs have been shown to act as molecular sponges for miRNAs and play crucial roles in skeletal muscle development across various species. For example, circTMTC1 inhibits the differentiation of chicken skeletal muscle satellite cells by acting as a molecular sponge for miR-128-3p (Shen et al., 2019). circPSME4 interacts with ssc-miR-181d-3p, thereby modulating *MYOD1* expression and influencing porcine myoblast proliferation and differentiation (Zeng et al., 2023). In cattle, circRILPL1 functions as a molecular sponge for miR-145, regulating the *IGF1R* gene and diminishing miR-145′s suppression of the PI3K/AKT pathway, thus facilitating myoblast proliferation (Shen et al., 2021). These observations highlight the conserved yet diverse roles of circular RNAs (circRNAs) in the regulation of skeletal muscle across different species.

In this study, the target prediction result of miR-22-5p indicate that several of the target genes *(MYL9, GRB2, CLCN1)* for miR-22-5p are associated with muscle development. For instance, *MYL9* acts as a regulatory light chain in myosin, aiding ATP hydrolysis to promote actin movement and significantly contributing to skeletal muscle growth and development (Heissler and Sellers, 2016; Sitbon et al., 2020). Research has demonstrated that *GRB2* activates the Ras-MAPK signaling pathway through its interaction with the Met receptor, thereby promoting the proliferation and differentiation of myoblasts (Maina et al., 1996; Mitra and Thanabalu, 2017). Moreover, the *CLCN1* gene encodes a chloride ion channel that is essential for maintaining the resting membrane potential of skeletal muscle and preventing muscle stiffness (Kino et al., 2009).

This study provides novel perspectives on how circFBLN2 and miR-22-5p regulate DPMs. These findings could potentially enhance muscle growth and yield in the poultry industry. circFBLN2/miR-22-5p/MEF2C regulatory network could potentially be leveraged to optimize muscle growth in commercial poultry breeds. Identification of key regulatory elements could facilitate the development of genetic markers for selective breeding programs aimed at improving muscle yield.

Several studies focusing on primary chicken myoblasts have highlighted the significant roles of circRNA and miRNA in the development of skeletal muscle (Cai et al., 2022; Wu et al., 2023; Jiao et al., 2024). The current research identifies the functions of circFBLN2/miR-22-5p in primary myoblasts from duck embryos, reinforcing its critical importance in the development of duck skeletal muscle. However, the roles of these molecules in vivo are yet to be fully understood. Future studies plan to utilize established protocols to create lentiviral vectors for circFBLN2 knockdown and overexpression. Additionally, in vivo transfection reagents or injectable miRNA products (agomiR and antagomiR) will be employed to manipulate miR-22-5p levels (Zhao et al., 2024). These substances are intended for injection into the allantoic vein of duck embryos at embryonic day 12, a stage during which myoblasts remain undifferentiated. Seven days post-injection, in vivo evaluations using tissue qRT-PCR, Western blotting, and HE staining of paraffin-embedded sections can be conducted to examine the impacts of circFBLN2 and miR-22-5p on duck embryonic skeletal muscle development. Moreover, these reagents can also be injected into the gastrocnemius muscle of 1-day-old ducklings to assess the regulatory effects of

circFBLN2 and miR-22-5p on skeletal muscle hypertrophy seven days after injection.

Conclusions

In summary, our research identifies a novel circular RNA, circFBLN2, associated with duck skeletal muscle development. circFBLN2 functions as a molecular sponge for miR-22-5p, inhibiting the proliferation and promoting the differentiation of duck primary myoblasts (DPMs) (Fig. 8). Our findings provide direct evidence for the ceRNA regulatory mechanism in DPMs and reveal the critical role of the circFBLN2/miR-22-5p/MEF2C axis in regulating DPMs proliferation and differentiation. Therefore, this study offers new insights into the regulatory mechanisms of duck skeletal muscle development. The circFBLN2/miR-22-5p/MEF2C axis may serve as a potential molecular target for augmenting duck skeletal muscle growth and development, with significant implications for enhancing poultry muscle growth and livestock productivity.

Declaration of generative AI and AI-assisted technologies in the writing process

During the preparation of this work, the authors used ChatGPT to spelling and grammar checks, as well as linguistic enhancement. After using ChatGPT, the authors reviewed and edited the content as needed and take full responsibility for the content of the publication.

Disclosures

The corresponding author declares no conflict of interest on behalf of all authors.

Acknowledgments

The financial support for this study was provided by several organizations. The National Natural Science Foundation of China contributed through grant number 32102541 and the Natural Science Foundation of Jiangxi Province supported the research with grant numbers 20212BAB215016 and 20232BAB205061. Additionally, funding was also received from the Technology System of the Modern Agricultural Poultry Industry of Jiangxi Province, under project JXARS-09.

Supplementary materials

Supplementary material associated with this article can be found, in the online version, at doi:10.1016/j.psj.2025.105063.

References

Adhikari, A., Kim, W., Davie, J., 2021. Myogenin is required for assembly of the transcription machinery on muscle genes during skeletal muscle differentiation. PLoS One 16, e0245618.
Allen, R.E., Boxhorn, L.K., 1989. Regulation of skeletal muscle satellite cell proliferation and differentiation by transforming growth factor-beta, insulin-like growth factor I, and fibroblast growth factor. J Cell Physiol 138, 311–315.
Ambros, V., 2004. The functions of animal microRNAs. Nature 431, 350–355.
Ballarino, M., Morlando, M., Fatica, A., Bozzoni, I., 2016. Non-coding RNAs in muscle differentiation and musculoskeletal disease. J. Clin. Invest. 126, 2021–2030.
Bartel, D.P., 2004. MicroRNAs: genomics, biogenesis, mechanism, and function. Cell 116, 281–297.
Betel, D., Koppal, A., Agius, P., Sander, C., Leslie, C., 2010. Comprehensive modeling of microRNA targets predicts functional non-conserved and non-canonical sites. Genome Biol, 11:R90.
Buckingham, M., Bajard, L., Chang, T., Daubas, P., Hadchouel, J., Meilhac, S., Montarras, D., Rocancourt, D., Relaix, F., 2003. The formation of skeletal muscle: from somite to limb. J. Anat. 202, 59–68.
Cai, B., Ma, M., Zhou, Z., Kong, S., Zhang, J., Zhang, X., Nie, Q., 2022. circPTPN4 regulates myogenesis via the miR-499-3p/NAMPT axis. J Animal Sci Biotechnol 13 (2).
Chen, B., Liu, S., Zhang, W., Xiong, T., Zhou, M., Hu, X., Mao, H., Liu, S., 2022. Profiling analysis of N6-methyladenosine mRNA methylation reveals differential m6A patterns during the embryonic skeletal muscle development of ducks. Animals 12, 2593.
Chen, J.F., Mandel, E..M., Thomson, J.M., Wu, Q., Callis, T.E., Hammond, S.M., Conlon, F.L., Wang, D.-Z., 2006. The role of microRNA-1 and microRNA-133 in skeletal muscle proliferation and differentiation. Nat. Genet. 38, 228–233.
Chen, L., Wang, C., Sun, H., Wang, J., Liang, Y., Wang, Y., Wong, G., 2021a. The bioinformatics toolbox for circRNA discovery and analysis. Brief. Bioinform. 22, 1706–1728.
Chen, M., Wei, X., Song, M., Jiang, R., Huang, K., Deng, Y., Liu, Q., Shi, D., Li, H., 2021b. Circular RNA circMYBPC1 promotes skeletal muscle differentiation by targeting MyHC. Mol Ther Nucleic Acids 24, 352–368.
Correia de Sousa, M., Gjorgjieva, M., Dolicka, D., Sobolewski, C., Foti, M., 2019. Deciphering miRNAs' Action through miRNA editing. Int J Mol Sci 20, 6249.
Gu, X., Wang, S., Li, D., Jin, B., Qi, Z., Deng, J., Huang, C., Yin, X., 2023. MicroRNA-142a-3p regulates neurogenic skeletal muscle atrophy by targeting Mef2a. Mol Ther Nucleic Acids 33, 191–204.
Gu, L., Xu, T., Huang, W., Xie, M., Sun, S., Hou, S., 2014. Identification and profiling of microRNAs in the embryonic breast muscle of pekin duck. PloS One 9, e86150.
Güller, I., Russell, A.P., 2010. MicroRNAs in skeletal muscle: their role and regulation in development, disease and function. J. Physiol. 588, 4075–4087.
Hansen, T.B., Jensen, T..I., Clausen, B.H., Bramsen, J.B., Finsen, B., Damgaard, C.K., Kjems, J., 2013. Natural RNA circles function as efficient microRNA sponges. Nature 495, 384–388.
Heissler, S.M., Sellers, J.R., 2016. Kinetic adaptations of myosins for their diverse cellular functions. Traffic 17, 839–859.
Helsten, T., Kato, S., Schwaederle, M., Tomson, B.N., Buys, T.P.H., Elkin, S.K., Carter, J. L., Kurzrock, R., 2016. Cell-cycle gene alterations in 4,864 tumors analyzed by next-generation sequencing: implications for targeted therapeutics. Mol. Cancer Ther. 15, 1682–1690.
Hu, Z., Cao, J., Zhang, J., Ge, L., Zhang, H., Liu, X., 2021. Skeletal muscle transcriptome analysis of Hanzhong Ma duck at different growth stages using RNA-seq. Biomolecules 11, 315.
Huang, J., Xiong, X., Zhang, W., Chen, X., Wei, Y., Li, H., Xie, J., Wei, Q., Zhou, Q., 2024. Integrating miRNA and full-length transcriptome profiling to elucidate the mechanism of muscle growth in muscovy ducks reveals key roles for miR-301a-3p/ANKRD1. BMC genomics 25, 340.
Hydbring, P., Malumbres, M., Sicinski, P., 2016. Non-canonical functions of cell cycle cyclins and cyclin-dependent kinases. Nat Rev Mol Cell Biol 17, 280–292.
Jiao, Z., Xie, T., Wang, X., Guo, D., Lin, S., An, L., Lin, J., Zhang, L., 2024. Novel circular RNA CircSLC2A13 regulates chicken muscle development by sponging MiR-34a-3p. J. Agric. Food Chem. 72, 15530–15540.
Khalid, T., Hdaifeh, A., Federighi, M., Cummins, E., Boué, G., Guillou, S., Tesson, V., 2020. Review of quantitative microbial risk assessment in poultry meat: the Central position of consumer behavior. Foods 9, 1661.
Kino, Y., Washizu, C., Oma, Y., Onishi, H., Nezu, Y., Sasagawa, N., Nukina, N., Ishiura, S., 2009. MBNL and CELF proteins regulate alternative splicing of the skeletal muscle chloride channel CLCN1. Nucleic Acids Res 37, 6477–6490.
Krüger, J., Rehmsmeier, M., 2006. RNAhybrid: microRNA target prediction easy, fast and flexible. Nucleic Acids Res 34, W451–W454.
Lehka, L., Rędowicz, M.J., 2020. Mechanisms regulating myoblast fusion: a multilevel interplay. Semin. Cell Dev. Biol. 104, 81–92.
Lei, Q., Hu, X., Han, H., Wang, J., Liu, W., Zhou, Y., Cao, D., Li, F., Liu, J., 2022. Integrative analysis of circRNA, miRNA, and mRNA profiles to reveal ceRNA regulation in chicken muscle development from the embryonic to post-hatching periods. BMC genomics 23, 342.
Li, C., Xiong, T., Zhou, M., Wan, L., Xi, S., Liu, Q., Chen, Y., Mao, H., Liu, S., Chen, B., 2020. Characterization of microRNAs during embryonic skeletal muscle development in the shan ma duck. Animals 10, 1417.
Li, X., Yang, L., Chen, L.-L., 2018. The biogenesis, functions, and challenges of circular RNAs. Mol. Cell 71, 428–442.
Li, Y., Yuan, P., Fan, S., Zhai, B., Li, S., Li, H., Zhang, Y., Li, W., Sun, G., Han, R., Tian, Y., Liu, X., Jiang, R., Li, G., Kang, X., 2022. miR-30a-3p can inhibit the proliferation and promote the differentiation of chicken primary myoblasts. Br. Poult. Sci. 63, 475–483.
Li, M., Zhang, N., Zhang, W., Hei, W., Cai, C., Yang, Y., Lu, C., Gao, P., Guo, X., Cao, G., Li, B., 2021. Comprehensive analysis of differentially expressed circRNAs and ceRNA regulatory network in porcine skeletal muscle. BMC genomics 22, 320.
Lin, Z., Xie, F., He, X., Wang, J., Luo, J., Chen, T., Jiang, Q., Xi, Q., Zhang, Y., Sun, J., 2024. A novel protein encoded by circKANSL1L regulates skeletal myogenesis via the Akt-FoxO3 signaling axis. Int. J. Biol. Macromol. 257, 128609.
Liu, C., Chen, L., 2022. Circular RNAs: characterization, cellular roles, and applications. Cell 185, 2016–2034.
Liu, H., Li, L., Chen, X., Cao, W., Zhang, R., Yu, H., Xu, F., He, H., Wang, J., 2011. Characterization of in vitro cultured myoblasts isolated from duck (Anas platyrhynchos) embryo. Cytotechnology 63, 399–406.
Liu, J., Liu, S., Zhang, W., Hu, X., Mao, H., Liu, S., Chen, B., 2023a. Transcriptome RNA sequencing reveals that circular RNAs are abundantly expressed in embryonic breast muscle of duck. Vet Sci 10, 75.
Liu, N., Nelson, B.R., Bezprozvannaya, S., Shelton, J.M., Richardson, J.A., Bassel-Duby, R., Olson, E.N., 2014. Requirement of MEF2A, C, and D for skeletal muscle regeneration. Proc Natl Acad Sci U S A 111, 4109–4114.
Liu, S., Wu, J., Zhang, W., Jiang, H., Zhou, Y., Liu, J., Mao, H., Liu, S., Chen, B., 2023b. Whole-transcriptome RNA sequencing uncovers the global expression changes and RNA regulatory networks in duck embryonic myogenesis. Int J Mol Sci 24, 16387.

Livak, K.J., Schmittgen, T.D., 2001. Analysis of relative gene expression data using real-time quantitative PCR and the 2(-Delta Delta C(T)) method. Methods 25, 402–408.
Lv, W., Yu, M., Su, Y., 2022. miR-22-5p regulates the self-renewal of spermatogonial stem cells by targeting EZH2. Open Med 17, 556–565.
Maina, F., Casagranda, F., Audero, E., Simeone, A., Comoglio, P.M., Klein, R., Ponzetto, C., 1996. Uncoupling of Grb2 from the met receptor in vivo reveals complex roles in muscle development. Cell 87, 531–542.
Malumbres, M., Barbacid, M., 2009. Cell cycle, CDKs and cancer: a changing paradigm. Nat Rev Cancer 9, 153–166.
Mitra, P., Thanabalu, T., 2017. Myogenic differentiation depends on the interplay of Grb2 and N-WASP. Biochim Biophys Acta Mol Cell Res 1864, 487–497.
Mo, M., Zhang, Z., Wang, X., Shen, W., Zhang, L., Lin, S., 2023. Molecular mechanisms underlying the impact of muscle fiber types on meat quality in livestock and poultry. Front Vet Sci 10, 1284551.
Nam, J.W., Rissland, O..S., Koppstein, D., Abreu-Goodger, C., Jan, C.H., Agarwal, V., Yildirim, M.A., Rodriguez, A., Bartel, D.P., 2014. Global analyses of the effect of different cellular contexts on microRNA targeting. Mol. Cell 53, 1031–1043.
Rogg, E.M., Abplanalp, W..T., Bischof, C., John, D., Schulz, M.H., Krishnan, J., Fischer, A., Poluzzi, C., Schaefer, L., Bonauer, A., Zeiher, A.M., Dimmeler, S., 2018. Analysis of cell type-specific effects of MicroRNA-92a provides novel insights into target regulation and mechanism of action. Circulation 138, 2545–2558.
van Rooij, E., Liu, N., Olson, E.N., 2008. MicroRNAs flex their muscles. Trends Genet 24, 159–166.
Scanes, C.G., Harvey, S.., Marsh, J.A., King, D.B., 1984. Hormones and growth in poultry. Poult. Sci. 63, 2062–2074.
Schneider, C.A., Rasband, W..S., Eliceiri, K.W., 2012. NIH image to ImageJ: 25 years of image analysis. Nat. Methods 9, 671–675.
Shen, X., Liu, Z., Cao, X., He, H., Han, S., Chen, Y., Cui, C., Zhao, J., Li, D., Wang, Y., Zhu, Q., Yin, H., 2019. Circular RNA profiling identified an abundant circular RNA circTMTC1 that inhibits chicken skeletal muscle satellite cell differentiation by sponging miR-128-3p. Int. J. Biol. Sci. 15, 2265–2281.
Shen, X., Tang, J., Jiang, R., Wang, X., Yang, Z., Huang, Y., Lan, X., Lei, C., Chen, H., 2021. CircRILPL1 promotes muscle proliferation and differentiation via binding miR-145 to activate IGF1R/PI3K/AKT pathway. Cell Death Dis 12, 142.
Shi, M., Yang, S., Zhao, X., Sun, D., Li, Y., Yang, J., Li, M., Cai, C., Guo, X., Li, B., Lu, C., Cao, G., 2024. Effect of LncRNA LOC106505926 on myogenesis and lipogenesis of porcine primary cells. BMC Genomics 25, 530.
Siracusa, J., Koulmann, N., Banzet, S., 2018. Circulating myomiRs: a new class of biomarkers to monitor skeletal muscle in physiology and medicine. J Cachexia Sarcopenia Muscle 9, 20–27.
Sitbon, Y.H., Yadav, S.., Kazmierczak, K., Szczesna-Cordary, D., 2020. Insights into myosin regulatory and essential light chains: a focus on their roles in cardiac and skeletal muscle function, development and disease. J Muscle Res Cell Motil 41, 313–327.
Sun, D., An, J., Cui, Z., Li, J., You, Z., Lu, C., Yang, Y., Gao, P., Guo, X., Li, B., Cai, C., Cao, G., 2022. CircCSDE1 Regulates proliferation and differentiation of C2C12 myoblasts by sponging miR-21-3p. Int J Mol Sci 23, 12038.
Szabo, L., Salzman, J., 2016. Detecting circular RNAs: bioinformatic and experimental challenges. Nat. Rev. Genet. 17, 679–692.
Tajsharghi, H., Oldfors, A., 2013. Myosinopathies: pathology and mechanisms. Acta Neuropathol 125, 3–18.
Tian, W., Liu, Y., Zhang, W., Nie, R., Ling, Y., Zhang, B., Zhang, H., Wu, C., 2023. CircDOCK7 facilitates the proliferation and adipogenic differentiation of chicken abdominal preadipocytes through the gga-miR-301b-3p/ACSL1 axis. J. Anim. Sci. Biotechnol. 14, 91.
Treiber, T., Treiber, N., Meister, G., 2019. Regulation of microRNA biogenesis and its crosstalk with other cellular pathways. Nat. Rev. Mol. Cell Biol. 20, 5–20.
Velleman, S.G., 2019. Recent developments in breast muscle myopathies associated with growth in poultry. Annu. Rev. Anim. Biosci. 7, 289–308.
Wang, S., Cao, X., Ge, L., Gu, Y., Lv, X., Getachew, T., Mwacharo, J.M., Haile, A., Sun, W., 2022. MiR-22-3p inhibits proliferation and promotes differentiation of skeletal muscle cells by targeting IGFBP3 in Hu sheep. Animals 12, 114.
Wang, H., Wang, B., Zhang, A., Hassounah, F., Seow, Y., Wood, M., Ma, F., Klein, J.D., Price, S.R., Wang, X.H., 2019. Exosome-mediated miR-29 transfer reduces muscle atrophy and kidney fibrosis in mice. Mol Ther 27, 571–583.
Wood, D.J., Endicott, J.A., 2018. Structural insights into the functional diversity of the CDK-cyclin family. Open Biol 8, 180112.
Wu, N., Gu, T., Lu, L., Cao, Z., Song, Q., Wang, Z., Zhang, Y., Chang, G., Xu, Q., Chen, G., 2019. Roles of miRNA-1 and miRNA-133 in the proliferation and differentiation of myoblasts in duck skeletal muscle. J. Cell. Physiol. 234, 3490–3499.
Wu, Y., Zhao, J., Zhao, X., He, H., Cui, C., Zhang, Y., Zhu, Q., Yin, H., Han, S., 2023. CircLRRFIP1 promotes the proliferation and differentiation of chicken skeletal muscle satellite cells by sponging the miR-15 family via activating AKT3-mTOR/p70S6K signaling pathway. Poult. Sci. 102, 103050.
Xu, J., Li, C., Kang, X., 2023. The epigenetic regulatory effect of histone acetylation and deacetylation on skeletal muscle metabolism-a review. Front Physiol 14, 1267456.
Yan, H., Gao, Y., Ding, Q., Liu, J., Li, Y., Jin, M., Xu, H., Ma, S., Wang, X., Zeng, W., Chen, Y., 2019. Exosomal micro RNAs derived from dermal papilla cells mediate hair follicle stem cell proliferation and differentiation. Int J Biol Sci 15, 1368–1382.
Yasmeen, S., Kaur, S., Mirza, A.H., Brodin, B., Pociot, F., Kruuse, C., 2019. miRNA-27a-3p and miRNA-222-3p as novel modulators of phosphodiesterase 3a (PDE3A) in cerebral microvascular endothelial cells. Mol. Neurobiol. 56, 5304–5314.
Yu, Y., Du, H., Wei, S., Feng, L., Li, J., Yao, F., Zhang, M., Hatch, G.m., Chen, L., 2018. Adipocyte-derived exosomal MiR-27a induces insulin resistance in skeletal muscle through repression of pparγ. Theranostics 8, 2171–2188.
Zammit, P.S., 2017. Function of the myogenic regulatory factors Myf5, MyoD, myogenin and MRF4 in skeletal muscle, satellite cells and regenerative myogenesis. Semin. Cell Dev. Biol. 72, 19–32.
Zeng, M., Yan, S., Yang, P., Li, Q., Li, J., Fan, X., Liu, X., Yao, Y., Wang, W., Chen, R., Han, G., Yang, Y., Tang, Z., 2023. Circular RNA transcriptome across multiple tissues reveal skeletal muscle-specific circPSME4 regulating myogenesis. Int. J. Biol. Macromol. 251, 126322.
Zhang, M., Zhang, L., Hei, R., Li, X., Cai, H., Wu, X., Zheng, Q., Cai, C., 2021. CDK inhibitors in cancer therapy, an overview of recent development. Am J Cancer Res 11, 1913–1935.
Zhao, X., Tang, S., Lei, Z., Shen, X., Zhang, Y., Han, S., Yin, H., Cui, C., 2024. circAGO3 facilitates NF-κb pathway-mediated inflammatory atrophy in chicken skeletal muscle via the miR-34b-5p/TRAF3 axis. Int J Biol Macromol 283, 137614.
Zhao, J., Zhao, X., Shen, X., Zhang, Y., Zhang, Y., Ye, L., Li, D., Zhu, Q., Yin, H., 2022. CircCCDC91 regulates chicken skeletal muscle development by sponging miR-15 family via activating IGF1-PI3K/AKT signaling pathway. Poult. Sci. 101, 101803.